HiSST: International Conference on
High-Speed Vehicle Science Technology
26–29 November 2018, Moscow, Russia

# The performance of heat-resistant heterophase silicide coatings in hypersonic air-plasma flows

*Astapov A.N.[1], Zhestkov B.E.[2], Lifanov I.P.[1], Terentieva V.S.[1]*

*[1] Moscow Aviation Institute (National Research University),*
*125993, Russia, Moscow, Volokolamskoe shosse, 4*
*[2] Central Aerohydrodynamic Institute named after prof. N.E. Zhukovsky,*
*140180, Russia, Moscow region, Zhukovsky, st. Zhukovsky, 1*

## Abstract

The degradation processes of structure of system Si-$TiSi_2$-$MoSi_2$-$TiB_2$ heat resistant coating in hypersonic air plasma flows were studied. It is established that the working capacity of the coating at temperatures on the surface of $T_w \leq 1820 \div 1830$°C is provided by the structural-phase state of its micro composite base layer and by the formation on the surface of a passivating heterogeneous protective film based on borosilicate glass film reinforced with rutile microneedles. The mechanism of degeneration of the coating at $T_w \geq 1850 \div 1860$°C consists of the erosion entrainment of the oxide film combined with generation and growth of gas-filled cavities at the interface «main coating layer – oxide film». When the saturated vapor pressure of the gaseous oxidation products (SiO, CO) exceeds the pressure values of the external environment, the integrity of the oxide film is broken, and the oxidation process goes into the active stage. The coating is designed to protect highly refractory materials against high temperature corrosion and erosion in oxygen containing gas flows.

**Keywords**: *heat-resistant coating, protection from oxidation, erosion, hypersonic flow, fire bench tests.*

## Nomenclature

EDS – Energy dispersive spectrometer
SEM – Scanning electron microscope
XRD – X-ray diffraction analysis

## 1. Introduction

There is a vital problem of protecting carbon-carbon and carbon – ceramic structural materials from high temperature oxidation and erosion at atmospheric flights with speed, exceeding Mach 5. There are several ways of providing this protection: inhibition of composites matrix [1, 2]; application of heat-resistant coatings on reinforcing fibers [3, 4]; but the most effective is application of coatings on the working surfaces of parts contacting with oxidizing media [5-10]. The study of the world practice in field of creation of heat-resistant coatings has shown that currently the silicide systems are most useful [3, 5-8].

This work is a continuation of the systematic studies in field of heterophase heat-resistant coatings of the Si-$TiSi_2$-$MoSi_2$-$TiB_2$ system conducted at the Moscow Aviation Institute (National Research University) [9, 10]. The principal difference of these coatings from the known ones is the microcomposition structure in form of refractory framework made of disilicide phases ($Ti_xMo_{1-x}Si_2$ ($0.1 < x < 0.87$), $TiSi_2$) and titanium diboride $TiB_2$, inside which is a relatively low-melting (comparing to operating temperature) eutectics (Si + disilicides), which acts as a self-healing structural component. This structure provides increased resistance to erosion and thermal shocks, the protection of sharp edges, and performance in conditions of short-term (up to 15÷20 seconds) temperature casts up to 2100÷2150°C. This heterophase material assembles itself after deposition during high-temperature interaction with oxygen-containing media in a multilayer multifunctional

coating. The properties of such coatings on carbon-ceramic composites of C-SiC class, attained thus far: the protective ability in hypersonic high-enthalpy air-plasma flows at temperatures on the surface of the coating $T_w$ = 1700°C is no less than 3600 seconds; at $T_w$ = 1800°C - not less than 900 seconds; at $T_w$ = 1900°C - not less than 200 seconds, at $T_w$ = 2000°C - not less than 60 seconds, at $T_w$ = 2100°C - not less than 20 seconds. The coatings provide low values of catalytic activity of the surface (the rate constant for the heterogeneous recombination of nitrogen and oxygen atoms is $K_w$ = 4÷6 m/s [11]), satisfactory characteristics of the emissivity ($\varepsilon \approx 0.7$ [12]), self-healing of technological and operational defects (∅ ≤ 0.6 mm ) and protection of sharp edges of parts (R ≥ 0.5 mm).

The present work investigates the mechanism of destruction of coatings of this system on C-SiC under conditions of stepwise heating of the surface by the hypersonic flow of air plasma in a wide range of temperatures up to $T_w$ = 1900÷1950°C in order to further enhance the functional properties of protective coatings and extend the temperature-time limits of their performance. Chemical composition of the coating lies in the concentration intervals established in patent [9]. The exact composition is know-how and for this reason is not disclosed.

## 2. Materials and research methods

As the initial components of the alloy for coating, we used powders of technical silicon of the KR00 brand, titanium of the PTOM-1 brand, molybdenum of the PM-99.95 brand, and boron of the amorphous B-99A brand. The powders were mixed in a ball mill in steel drums using hard alloy grinding bodies and pressed into cylindrical samples with a diameter of 18 mm and a height of 15 mm on a ZDM 50E hydraulic press with a force of 25 tons. Melting was performed in a suspended state in an atmosphere of 7.0 helium in an induction ETM-27 furnaces. To eliminate segregation, the ingots were annealed in a vacuum furnace of a mine type SSHVE-1.2.5/25 I2 at 1100°C for 5 h with a residual pressure of gases in the chamber 5÷6 MPa. The preparation of the powder was carried out by crushing the ingots in the same press with a force of 15 tons, followed by grinding in a ball mill with steel balls with a hardness of HRC = 58÷62 to a dispersity of ≤ 20 μm.

The coating was formed by the method of slip-firing fusion. As a substrate, sample discs with a diameter of 30 mm and 8.5 mm thickness of C-SiC class carbon-ceramic composite were used. Ethyl silicate was used as a binder in the slip suspension, and the resulting powder of an alloy of the Si-$TiSi_2$-$MoSi_2$-$TiB_2$ system was used as a filler. Slip layers were applied with a brush on all surfaces and edges of the samples. Drying was performed at a temperature of 80°C for 30 minutes. The firing was carried out in a SSHVE-1.2.5/25 I2 vacuum furnace until the deposited layer is melted and a compact coating is formed.

The chemical composition of the initial components, the resulting alloy, the powder, and the coating was studied by X-ray fluorescence analysis on an ARL OPTIM'X wave spectrometer from Thermo Scientific. The phase composition was determined by X-ray diffraction analysis (XRD) on an ARL X'tra diffractometer from Thermo Scientific. The study of the dispersion of the powder, the microstructure of the alloy and the coating was carried out on a Carl Zeiss EVO-40 scanning electron microscope (SEM) equipped with an energy dispersive spectrometer (EDS) for X-Max Oxford Instruments microanalysis. The samples were manufactured on high-precision equipment from Struers.

Gas dynamic bench tests were performed at NIO-8 Central Aerohydrodynamic Institute named after prof. N.E. Zhukovsky on the high-temperature wind tunnel VAT-104, equipped with an induction plasma torch with a capacity of 240 kW. Equipment and methods for conducting fire experiments are described in detail in [11, 12]. The processes of thermochemical interaction of samples with hypersonic streams of air plasma were modeled (for the conditions of entry of promising returnable aircraft into the Earth's atmosphere). The parameters of the air plasma were in the range: flow rate of 4.3÷4.5 km/s (Mach number $M$ = 5.5÷6.0); enthalpy of flow 40÷45 MJ/kg; braking temperature of flow 10,000°C; gas pressure in front of the samples 1.5÷3.3 kPa; the degree of air dissociation in the stream is 80÷90%; the degree of ionization is about 1%. The distance from the exit section of the nozzle to the front surface of the models in all experiments was 30 mm. The temperatures $T_w$ reached on the face of the samples during the tests were measured with a VS-CTT-285/E/P-2001 pyrometer at a wavelength of 890 nm and a VS-415U Tandem thermal imager at a wavelength of 650 nm taking into account the spectral degree of blackness of the coating, which was taken equal to

ε = 0,7 [12]. From the back of the samples, the temperature was controlled by thermocouples VR 5/20. Samples were weighed on an AND GR-202 analytical balance with an accuracy of $10^{-4}$ g.

## 3. Research results and discussion

### 3.1. Phase composition and coating structure of the system Si-$TiSi_2$-$MoSi_2$-$TiB_2$

According to the X-ray diffraction analysis, the phase composition of the coating is presented (in descending order, mol. %): $Ti_xMo_{1-x}Si_2$ (mainly $Ti_{0.8}Mo_{0.2}Si_2$, $Ti_{0.7}Mo_{0.3}Si_2$ and $Ti_{0.4}Mo_{0.6}Si_2$), $TiB_2$, $TiSi_2$, Si and SiC. The results of structural studies (according to SEM and EDS) showed that the disilicide phases ($Ti_xMo_{1-x}Si_2$, $TiSi_2$) are skeletal, the eutectic based on silicon (Si + $Ti_xMo_{1-x}Si_2$ + $TiSi_2$) is inside a kind of dendritic-cellular framework formed by these disilicides. Titanium diboride $TiB_2$ is represented by regular-cut crystals, evenly distributed in the coating volume.

### 3.2. Investigation of coating behavior under stepped heating with a hypersonic flow of air plasma

Investigation of coated samples behavior under heating by a hypersonic flow of air plasma was performed at a constant power of plate supply of an induction plasmatron $W_a$ = 202±2 kW. The samples were studied over a wide temperature range, up to $T_w$ = 1900÷1950°C, and were kept at these temperatures for no less than 360±10 s. Increasing of the average temperature of sample surfaces in the course of fire tests was performed by stepped pressure growing in the heater settling chamber $P_0$ from 8 up to 25 kPa. Transfer to the next pressure level was made at 250, 390, 510, 630, 750, 870, 970, 1040, 1125 and 1190 seconds from the beginning of experiments. Three similar samples were studied under the above conditions. A good reproducibility of experimental data was established. This indicates identity of physico-chemical processes occurring in a coating that interacts with a plasma flow as well as a small value of random errors.

Figure 1*a* presents a typical mode of gas-dynamic testings of samples and the achieved temperature level. Symbolic notations of the curves are: **1** – temperature at the sample front face in the vicinity of the critical point (over the area ~15 mm in diameter), $T_w$; **2** – power of the generator plate supply, $W_a$; **3** – stagnation pressure in the heater settling chamber, $P_0$; **4** – temperature at the sample backside at the critical point, $T_w$. A typical appearance of the samples front faces after their removal from testing is given in Fig. 1*b*. The average sample mass loss was 390±65 g/(m$^2$·h).

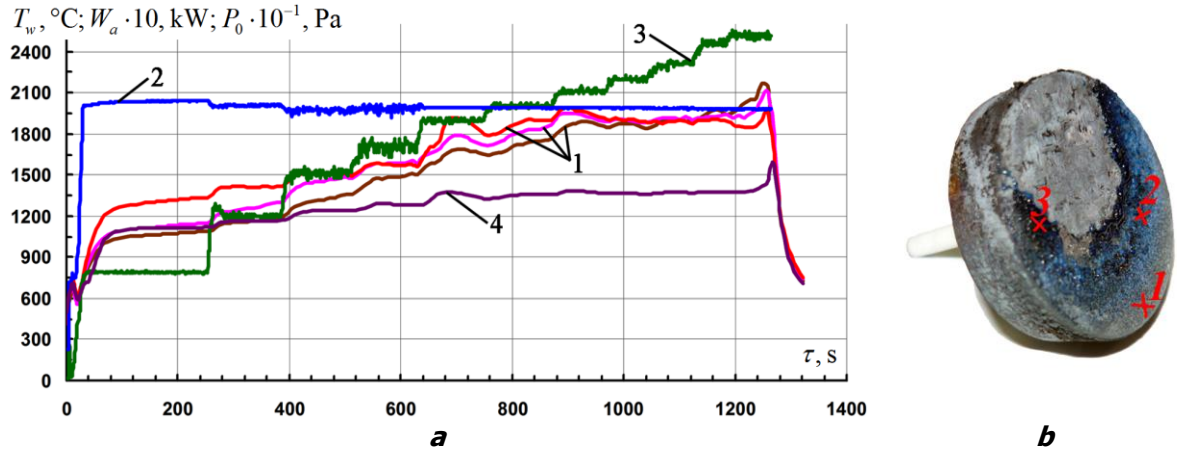


***a*** ***b***

**Fig. 1.** Typical gas-dynamic test mode for samples of C-SiC class with a coating of the Si-$TiSi_2$-$MoSi_2$-$TiB_2$ system: *a* - change of the mode parameters over time; *b* - a typical appearance of the front surface of the samples after testing

The character of the temperature curves **1** in Fig. 1*a* depending on the increasing with time stepped stagnation pressure **3** indicates predominance of the rate of low-catalytic oxide film formation at the coating surface over its sublimation under low external pressure (the flow pressure before the samples $P_w$ = 1.5÷3.3 kPa). This fact is confirmed by a regular decrease of the sustained radiation-equilibrium temperature of sample surface within 40÷60 s after regular transition to the next pressure step. Formation of a film (based on amorphous silica) of sufficient thickness in the

mentioned time interval leads to decrease of coating surface catalysity relative to the reactions of heterogeneous recombination of atoms of dissociated and partly ionized air (O, N, $O_2$, $N_2$, NO, $O^+$, $N^+$, $NO^+$ and $e^-$) and, therefore, to reduction of coating temperature [11, 13]. One can observe this especially clearly after the stepped pressure transitions in 630, 870, 970 and 1040 seconds from the start of firing experiments (Fig. 1*a*). Thus temperature value at the critical point drops from $T_w$ = 1900°C on 680 second of testing to $T_w$ = 1800°C on 745 second of testing at a constant pressure $P_0$ = 19 kPa; from $T_w$ = 1990°C on 900 second of testing to $T_w$ = 1915°C on 965 second of testing at a constant pressure $P_0$ = 21 kPa, etc.

It should be noted that, as pressure in the settling chamber increased to $P_0$ = 25 kPa, an abrupt uncontrolled growth of temperature at the sample front face surfaces (from $T_w$ ~ 1950°C up to $T_w$ ~ 2200°C) was registered on 1190 s from the start of firing experiments (Fig. 1*a*). As this temperature was achieved, the samples were removed from testing for examination. It can be seen from the photography in Fig. 1*b* that the C-SiC substrate is exposed in the center of flow action (a gray spot at the sample upper part), i.e., the coating is entirely absent. In outward appearance, the coating remained integral far from the center of action. However, presence of areas of different colors (black, blue and gray) indicates different degrees of coating degradation from the area of plasma flow localization through the outer regions.

Not the least of the facts is that in the present experiments the samples front faces were placed at a distance of 30 mm from the exit section of the aerodynamic tube nozzle, while the previous samples were tested at 70÷100 mm from the nozzle section [10-12]. Such a reduction of the distance led to appearance of a considerable temperature gradient over the sample surface in the course of testing. This is because of decreasing of the area of disturbed flow of air plasma, increasing of steepness of the shock wave front and growth of maximal temperature in the flow core (and consequently the gradient of heat flow density over the jet diameter). Presence of temperature gradient over the sample surface made it possible to separate out the areas far from the center of flow action where $T_w$ did not exceed 1820÷1830°C, 1850÷1860°C and 1890÷1900°C for 300÷350 s. The structural-phase investigations of coating in those areas made it possible to get additional information on operating capacity of coating and degree of its structure degradation at different temperatures.

### 3.3. Investigation of coating after action of a hypersonic flow of air plasma

The X-ray diffraction analysis of the sample face surfaces far from the center of flow action ($T_w$ = 1820÷1830°C) showed (Fig. 2*a*) that, in addition to a set of reflections that are characteristic of the initial coatings, a wide halo at 2θ = 22° (corresponding to amorphous $SiO_2$) and peaks related to rutile $TiO_2$ were observed. The proportion between the phases of the coating main layer (under the oxide film) practically had no changes as compared to the initial state. This indicates high thermo-chemical stability and low degree of coating structure degradation at the mentioned temperatures, as well as maintenance in total of coating protective properties after the considered interaction with a hypersonic flow of air plasma.

A considerable decrease of both free silicon amount (Fig. 2*a*) and the eutectic structural component of the coating main layer (that is responsible for self-healing of defects) occurs at approaching to the center of flow action and increasing of operating temperatures at the sample surface to $T_w$ = 1890÷1900°C. Besides, a considerable amount of lower silicides $Ti_5Si_3$ and $Mo_5Si_3$ (that apparently are formed due to silicon consumption from higher silicides at their oxidation) is registered. Also, a sharp increase in the intensity of diffraction reflexes from the substrate (SiC phase) is noted. This indicates a thinning of the coating and/or the existence of emptiness in its structure. Thus the phase composition of the coating main layer undergoes substantial quantitative and qualitative changes. Therefore the protective properties of coating become practically exhausted towards the end of testing at the mentioned temperatures.

It was of interest to investigate the structural-morphological features of coating areas subject to degradation of variable degrees during stand testings. The microstructures of coating surface after testing in the mode presented in Fig. 1*a* can serve as a typical example (see Fig. 3*a-c*). The areas of different colors were studied. Their centers are designated by "**×**" in Fig. 1*b* and enumerated: ***1*** (gray), ***2*** (blue) and ***3*** (black). The chemical composition of surface films in the neighborhood of the mentioned areas was averaged over the 300×300 μm region and is presented in Table 1.

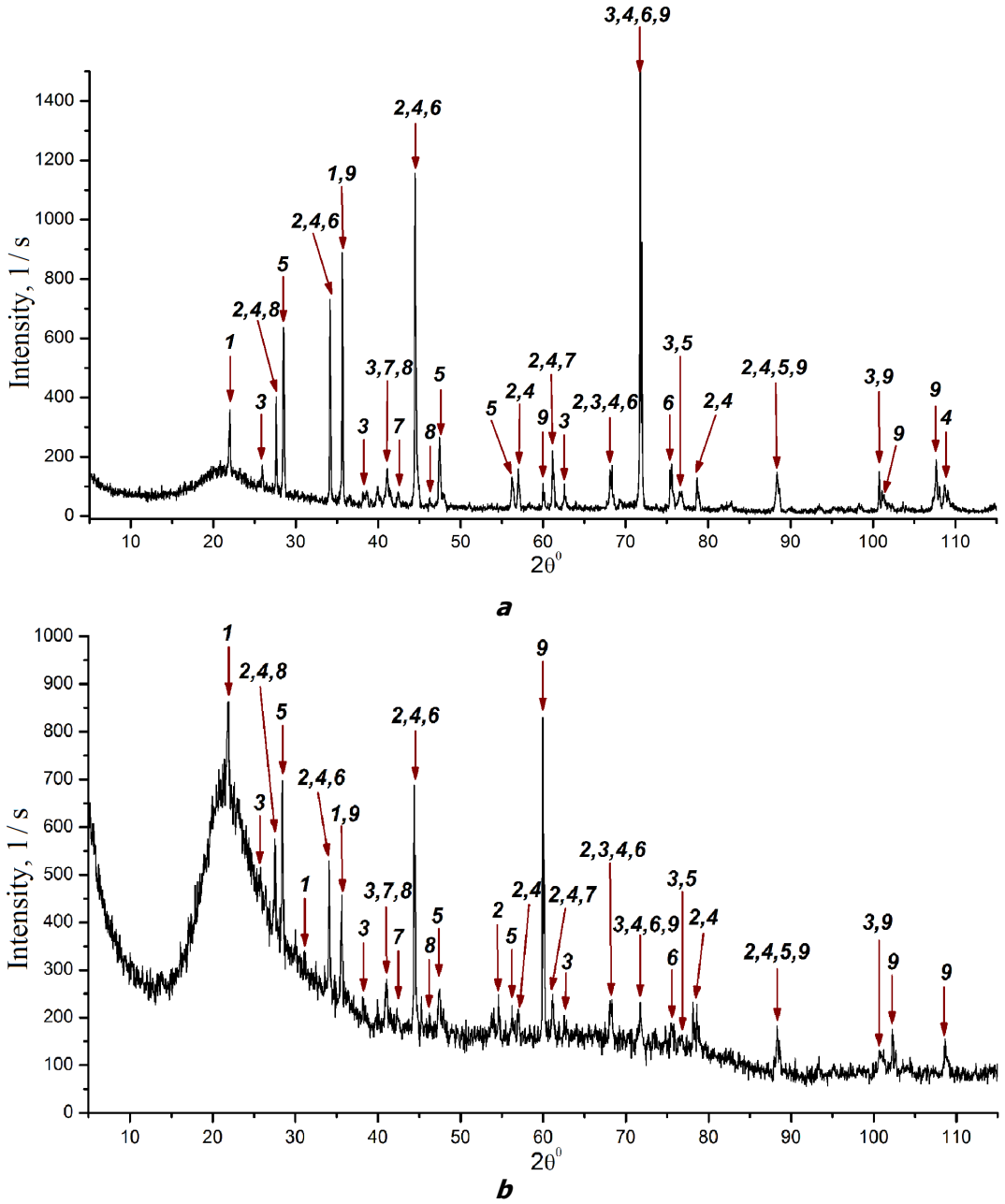


**Fig. 2.** X-ray patterns of the front surfaces of the samples after the fire tests when fixing various temperatures for 300÷350 s:
*a* – $T_w$ = 1820÷1830°C; *b*– $T_w$ = 1890÷1900°C. Phases: ***1*** – $SiO_2$; ***2*** – $TiO_2$; ***3*** – $Ti_xMo_{1-x}Si_2$; ***4*** – $TiB_2$; ***5*** – Si; ***6*** – $Mo_5Si_3$; ***7*** – $Ti_5Si_3$; ***8*** – $TiSi_2$; ***9*** – SiC

It was found that open pores, roughness and "laces" appear at initially smooth and relatively defectless surface because of coating interaction with a flow of air plasma at $T_w \geq 1850\div1860$°C. Those pores are not through. This is indirectly proved by carbon content in the surface layers (Table 1). Small amounts of carbon seem to relate to adsorption of hydrocarbon molecules at the sample surface (carbon deposit formation). The number and linear dimensions of pores and irregularities increase as the center of heat flow action is approached (Fig. 3*a-c*), while the chemical composition of oxide films remains the same on the average in the studied surface areas. Small variations of chemical composition in oxide films from regions of different colors seem to be due to errors of quantitative analysis of light elements (O, C, B) and to the effect of surface irregularities on the results of microanalysis. Therefore, one can conclude to a high probability that distinctions in oxide films color are most likely related to the state of their surface, number and size of the forming pores (the effect of visible light reflection), thickness and heterogeneity degree of the films themselves (the light interference effect).

It should be noted that the beginning of coating degradation is accompanied by appearance of bulges, dome-shaped puddles and gas-filled bubbles (Fig. 3*a*) (40÷60 μm in diameter and about 10÷15 μm in height). The intensity of their formation increases with temperature (Fig. 3*b,c*). Violation of coating continuity (and consequently reduction of its protective action) seems to result from break of the above formations and transition to the "boiling" mode.

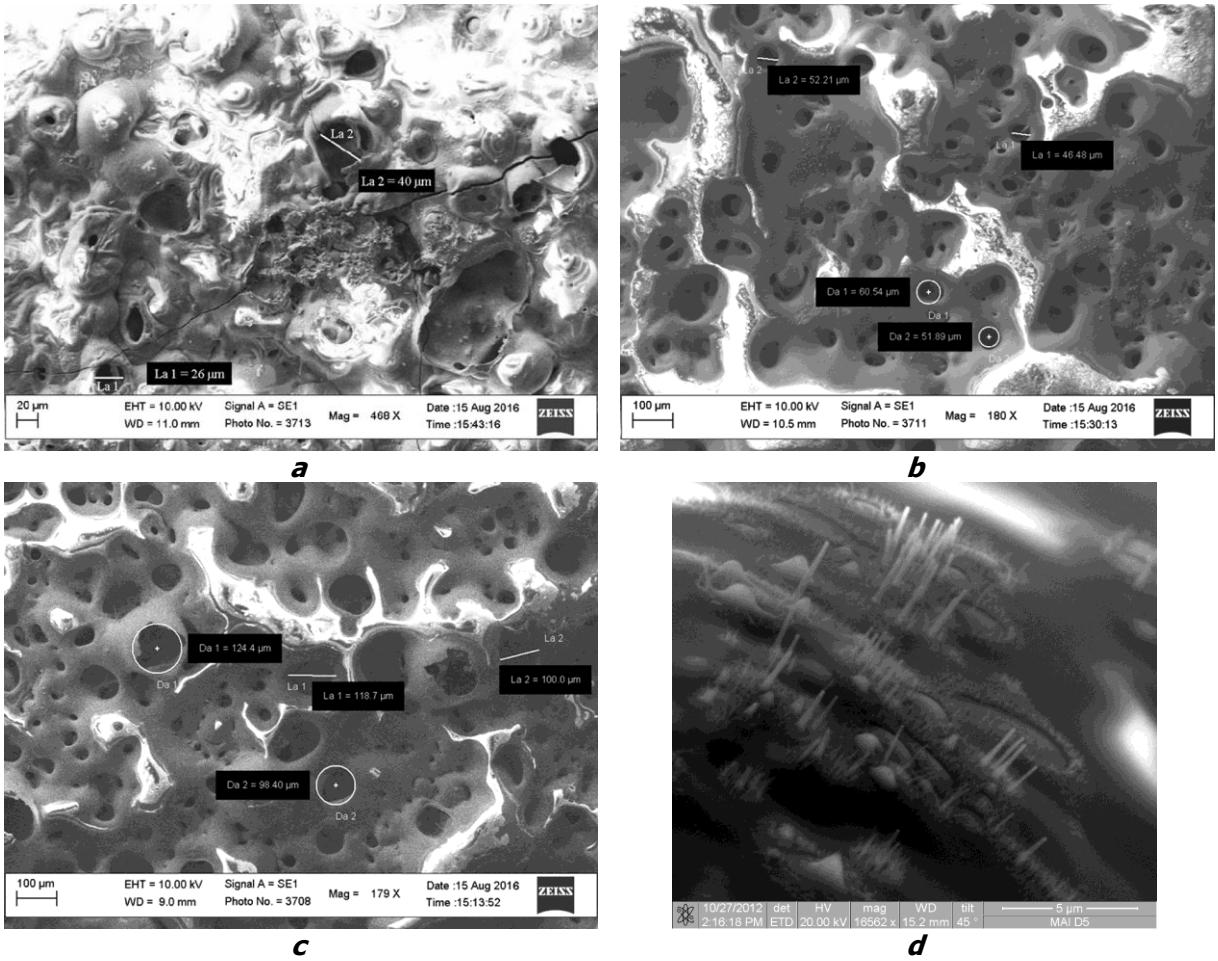


**Fig. 3.** Typical microstructure of individual regions of the coating surface after fire testing with parameters according to Fig. *1a*: *a* – *c* – regions *1* – *3* (according to numeration at Fig. 1*b*); *d* – surface of the heterophase oxide film with emerging $TiO_2$ needles after testing at $T_w \leq 1820 \div 1830$°C;
*a* – x468; *b* – x180; *c* – x179; *d* – x16562

**Table 1.** Chemical composition of the surface areas of the coating, marked in Fig. 1*b*

| Section | Chemical composition, at. % | | | | | |
|---|---|---|---|---|---|---|
| | O | Si | Ti | Mo | C | B |
| *1* | 68.28 | 28.25 | 1.36 | - | 2.11 | At the backround level |
| *2* | 71.38 | 25.61 | 0.78 | - | 2.23 | |
| *3* | 73.02 | 25.01 | 0.38 | 0.36 | 1.23 | |

Investigation of coating bulk oxidation was performed when studying slice cross-sections of the areas subject to different temperature actions in the course of firing testings. The typical microstructures of coating cross-sections in these areas are presented in Fig. 4. Here (from left to right): a resin - to keep the sample edges when polishing; an oxide film formed on the studied coating surface during its operation; the main layer of coating of the Si-$TiSi_2$-$MoSi_2$-$TiB_2$ system; a SiC barrier layer; carbon fibers in the SiC-matrix. One can see from Fig. 4 that thicknesses of the oxide areas essentially differ

in areas with different operating temperatures. To illustrate, the oxide film thickness is ~5÷10 μm in the areas heated to $T_w$ = 1820÷1830°C (Fig. 4*a*), ~20÷30 μm in the areas heated to $T_w$ = 1850÷1860°C (Fig. 4*b*) and ~90÷110 μm in the areas heated to $T_w$ = 1890÷1900°C (Fig. 4*c*). (The thickness values are given without regard for mechanical loss of some part of oxide films due to erosion when interacting with flows.) The thickness of the coating main (unoxidized) layer, on the contrary, decreases as operating temperatures grow, because more layer structural components are used up due to formation and growth of an oxide film. For the areas presented in Figs. 4*a*, 4*b* and 4*c*, the thickness of coating main layer is no more than 35÷40 μm, 15÷20 μm and 5÷10 μm, respectively. Figures 4*b* and 4*c* also demonstrate formation and development of gas-filled cavities in the bulk of coating oxide layer, while Fig. 4*d* demonstrates disruption of oxide film integrity because of breaking of the above cavities and passing of gaseous oxidation products outside.

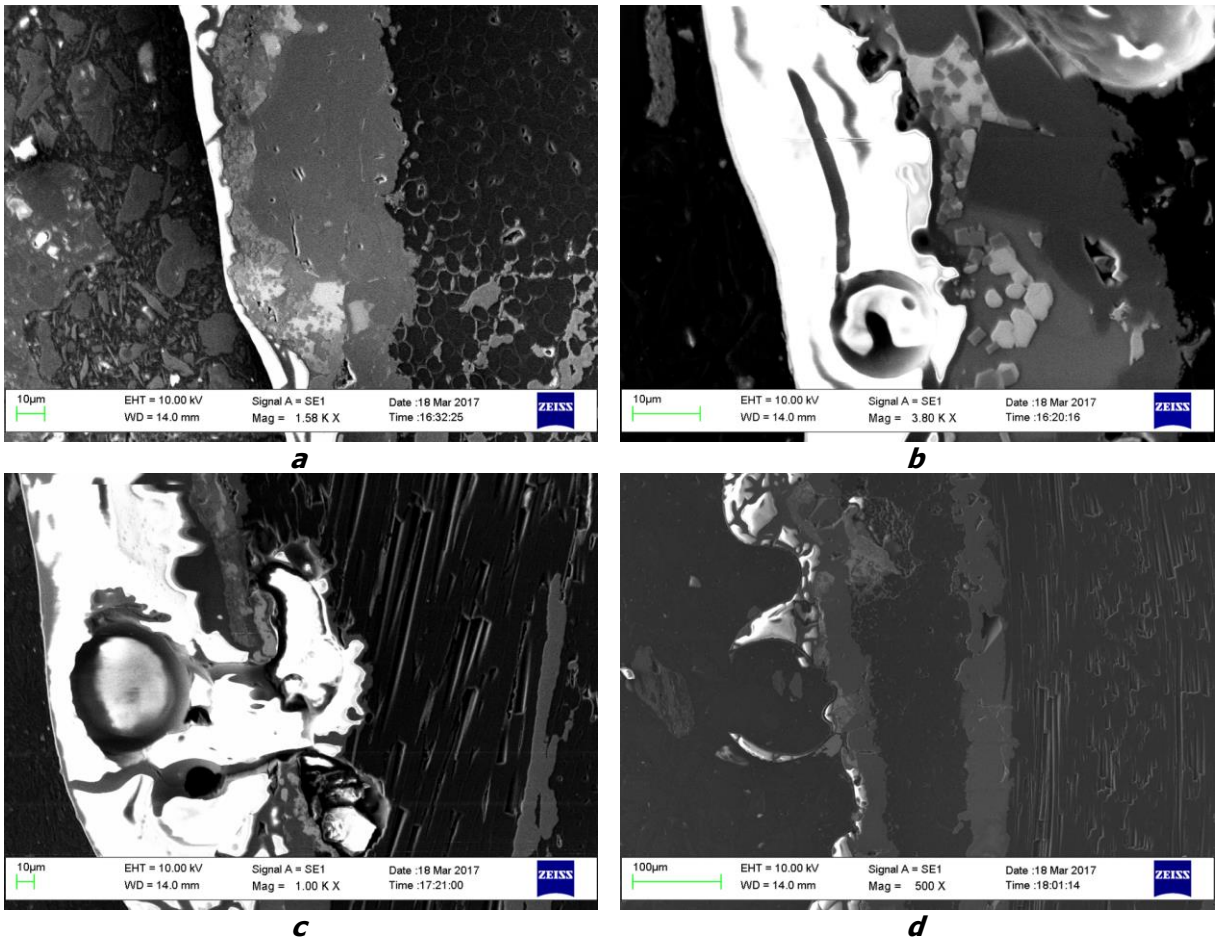


**Fig. 4.** Typical microstructure of the cross sections of the coating regions after fire tests with the fixation of various temperatures on the surface for 300 ÷ 350 s:
*a* – $T_w$ = 1820÷1830°C, x1580; *b* – $T_w$ = 1850÷1860°C, x3800;
*c* – $T_w$ = 1890÷1900°C, x1000; *d* – $T_w \geq$ 1900÷1950°C, x500

### 3.4. Operating capacity of coating and mechanism of its destruction in hypersonic flows of air plasma

An analysis of results obtained in the present paper, along with those of the previous studies [9-12], made it possible to state the following. Surface passivation that prevents development of an active oxidation in the coating bulk occurs under coating interaction with hypersonic flows of air plasma at temperatures up to $T_w$ = 1820÷1830°C.

The oxidation processes are given by the following reactions:

$$Si + O_2 \rightarrow SiO_2; \quad (1)$$

$$5MeSi_2 + 7O_2 \rightarrow 7SiO_2 + Me_5Si_3; \quad (2)$$

$$2SiC + 3O_2 \rightarrow 2SiO_2 + 2CO\uparrow; \quad (3)$$

$$2TiB_2 + 5O_2 \rightarrow 2TiO_2 + 2B_2O_3; \quad (4)$$

$$SiO_2 + B_2O_3 \rightarrow SiO_2 \cdot B_2O_3. \quad (5)$$

Formation of a $SiO_2$-based protective film occurs at oxidation of free silicon entering the composition of eutectic of the coating main layer as well as oxidation of higher silicides $MeSi_2$ ($Ti_xMo_{1-x}Si_2$, $TiSi_2$) and SiC that form a refractory frame (reactions 1–3, respectively). Simultaneous $TiB_2$ oxidation (reaction 4) and interaction of the oxidation products with $SiO_2$ result in formation of a heterogeneous protective film (Fig. 4*a*). It consists of both viscous glass $SiO_2 \cdot B_2O_3$ (reaction 5) and titanium oxide $TiO_2$ in the form of rutile. The latter does not mix with $SiO_2 \cdot B_2O_3$ and is an extensive net of randomly located microscopic needles (Fig. 3*d*). This leads to reinforcement of oxide film and thus to its additional increase of resistance to erosion loss in flows.

Besides, it is known that the systems demonstrating immiscibility are characterized by a considerable growth of liquidus temperature and increased viscosity. The latter feature reduces rate of oxygen diffusion through oxide film surface according to the Stokes-Einstein relationship [13]; it shows that diffusion permeability varies inversely with viscosity. Another potential advantage of increased viscosity on along with increased liquidus temperature is some reduction of saturated vapor pressure of heterogeneous silicate films as compared to pure $SiO_2$ oxide [13] that is formed at oxidation of single silicon-containing compounds (SiC, $Si_3N_4$, $MoSi_2$ et al.).

Increasing of operating temperatures at the surface up to $T_w$ = 1850÷1860°C and retardation of oxygen diffusion into the coating bulk through the growing heterogeneous oxide layer lead to (i) interaction of free silicon and SiC with $SiO_2$ film at its inner boundary and (ii) formation of gaseous products under the oxide film (at the Si-$SiO_2$ and SiC-$SiO_2$ boundaries) according to the following reactions:

$$Si + SiO_2 \rightarrow 2SiO\uparrow; \quad (6)$$

$$SiC + 2SiO_2 \rightarrow 3SiO\uparrow + CO\uparrow. \quad (7)$$

As a result, cavities filled with gases (predominantly silicon monoxide SiO) are formed under the oxide film (Fig. 4*b*). The lower is the oxygen partial pressure in the ambient, the more intense is the process of SiO formation [13]. The interaction of volatile silicon monoxide SiO with $O_2$ that is diffusing through the heterogeneous oxide film leads to increasing of $SiO_2$ film thickness from its lower boundary (Fig. 4*c*) according to the reaction:

$$2SiO\uparrow + O_2 \rightarrow 2SiO_2. \quad (8)$$

The reaction 8 makes a positive contribution to compensation of $SiO_2$ loss because of erosion loss from the surface streamlined with a hypersonic flow.

At further increasing of operating temperatures to $T_w \geq$ 1890÷1900°C, the gas bubbles are breaking because the pressure of saturated vapors of the formed gaseous products is higher than that of the ambient air. The gases "break" a viscous layer based on doped $SiO_2$, oxide film integrity is disrupted and intense oxidation of free silicon and SiC starts according to the reactions:

$$2Si + O_2 \rightarrow 2SiO\uparrow; \quad (9)$$

$$SiC + O_2 \rightarrow SiO\uparrow + CO\uparrow \quad (10)$$

That is, coating oxidation turns into the active phase. An ample blistering of coating (the "boiling" effect) is observed. It leads to instantaneous degradation of the oxide film (the "breaking from within" effect) (Fig. 4*d*). An absence of a film (based on amorphous silica) or its discontinuity in its turn results in increasing of coating surface catalysity relative to heterogeneous recombination reactions of air plasma atoms and, therefore, to additional surface heating [11].

It should be noted that the chemical reactions 1–4 and 8–10 are proceeding with participation of molecular oxygen. Its reactivity is much less than that of atomic oxygen. Presence of predominant amount of atomic oxygen in the air plasma flow (due to air dissociation in a shock wave before the samples) leads to acceleration of oxidation processes and increasing of oxidant diffusion permeability through a growing oxide layer.

Thus, the main reasons leading to loss of protecting antioxygenic functions by coating of the Si-$TiSi_2$-$MoSi_2$-$TiB_2$ system at surface temperatures $T_w \geq$ 1850÷1860°C under ambient pressure $P_w \leq$

0.1 atm. are erosion loss of oxide film as well as appearance, growth and breaking of gas-filled cavities.

We plan to direct our further investigations at improvement of chemical and phase compositions of the studied coatings aiming to form at their surfaces heterogeneous oxide films resistant to higher temperatures. The main problems to be solved are increasing of films viscosity (to reduce oxygen diffusion through them) and reduction of saturated vapor pressure at the "coating main layer–film" interface (to decrease sublimation processes and probability of disruption of films integrity in the course of appearance, growth and breaking of gas-filled cavities).

## 4. Conclusions

1. The results of firing gas-dynamic tests of samples from C-SiC protected by a coating of the Si-$TiSi_2$-$MoSi_2$-$TiB_2$ system are presented under conditions of stepwise surface heating up to $T_w \geq 1900 \div 1950$°C with hypersonic air plasma flow with $M = 5.5 \div 6.0$ and enthalpy up to 45 MJ/kg.

2. The working capacity of the coating at temperatures on the surface of $T_w \leq 1820 \div 1830$°C is ensured by the phase-structure state of its microcomposition base layer and the formation of a passivating heterogeneous protective film on the surface during operation of the borosilicate glass reinforced with microneedle titanium oxide in the form of rutile.

3. The mechanism of destruction of the coating at temperatures on the surface $T_w \geq 1850 \div 1860$°C lies in the erosion entrainment of the oxide film, generation and growth of cavities at the interface "main coating layer - oxide film" filled with volatile compounds (mainly SiO and CO). When the saturated vapor pressure of the oxidation products exceeds the ambient pressure values, the integrity of the oxide film is broken, the oxidation process goes into the active stage. Erosion and sublimation rates increase with increasing operating temperature and decreasing ambient pressure.

## Acknowledgements

The work was supported by the Russian Foundation for Basic Research (project code 17-08-01527-a).

## References

1. *Feng, Q., Wang, Z., Zhou, H.J. et al.* Microstructure analysis of $C_f$/SiC–ZrC composites in both fabrication and plasma wind tunnel testing processes // *Ceramics International*. 2014. Vol. 40. No. 1. Pp. 1199–1204. DOI: 10.1016/j.ceramint.2013.05.097.

2. *Uhlmann, F., Wilhelmi, C., Schmidt-Wimmer, S. et al.* Preparation and characterization of $ZrB_2$ and TaC containing $C_f$/SiC composites via Polymer-Infiltration-Pyrolysis process // *J. of the European Ceramic Society*. 2017. Vol. 37. No. 5. Pp. 1955–1960. DOI: 10.1016/j.jeurceramsoc.2016.12.048.

3. *Tkachenko, L.A., Shaulov, A.Yu., Berlin, A.A.* High-temperature protective coatings for carbon fibers // *Inorganic Materials*. 2012. Vol. 48. No. 3. Pp. 213–221. DOI: 10.1134/S0020168512030168.

4. *Xia, Ke-dong, Lu, Chun-xiang, Yang, Y.* Improving the oxidation resistance of carbon fibers using silicon oxycarbide coatings // *New Carbon Materials*. 2015. Vol. 30. No. 3. Pp. 236–243. DOI: 10.1016/S1872-5805(15)60188-3.

5. *Zmij, V.I., Rudenkyi, S.G., Shepelev, A.G.* Complex Protective Coatings for Graphite and Carbon-Carbon Composite Materials // *Materials Sciences and Applications*. 2015. Vol. 6. No. 10. Pp. 879–888. DOI: 10.4236/msa.2015.610090.

6. *Astapov, A.N., Terent'eva, V.S.* Review of domestic designs in the field of protecting carbonaceous materials against gas corrosion and erosion in high-speed plasma fluxes // *Russian J. of Non-Ferrous Metals*. 2016. Vol. 57. No. 2. Pp. 157–173. DOI: 10.3103/S1067821216020048.

**7.** *Jin, X., Fan, X., Lu, C., Wang, T.* Advances in oxidation and ablation resistance of high and ultra-high temperature ceramics modified or coated carbon/carbon composites // *J. of the European Ceramic Society*. 2018. Vol. 38. No. 1. Pp. 1–28. DOI: 10.1016/j.jeurceramsoc.2017.08.013.

**8.** *Yurishcheva, A.A., Astapov, A.N., Lifanov, I.P., Rabinskiy, L.N.* High temperature coatings for oxidation and erosion protection of heat-resistant carbonaceous materials in high-speed flows // *Key Engineering Materials*. 2018. Vol. 771. Pp. 103–117. DOI: 10.4028/www.scientific.net/KEM.771.103.

**9.** *Terentieva, V.S., Bogachkova, O.P., Goriatcheva, E.V.* Method for protecting products made of a refractory material against oxidation, and resulting protected products. US Patent No 5677060; 14 October 1997.

**10.** *Astapov, A.N.* Heat-resistant non-fired repair coatings for protection of carbon-base materials // *Nanomechanics Science and Technology: An International Journal*. 2014. Vol. 5. No 4. Pp. 267–285. DOI: 10.1615/NanomechanicsSciTechnolIntJ.v5.i4.20.

**11.** *Zhestkov, B.E., Shtapov, V.V.* Investigation of material condition in a hypersonic plasma flow // *Zavodskaya Laboratoriya. Diagnostika Materialov*. 2016. Vol. 82. No. 12. Pp. 58–65 (in Russian).

**12.** *Zhestkov, B.E.* Investigation of thermo-chemical stability of heat-shielding materials // *Uchenye Zapiski TsAGI*. 2014. Vol. XLV. No. 5. Pp. 62–77 (in Russian).

**13.** *Opeka, M.M., Talmy, I.G., Zaykoski, J.A.* Oxidation-based materials selection for 2000 C + hypersonic aerosurfaces: Theoretical considerations and historical experience // *J. of Materials Science*. 2004. Vol. 39. No. 19. Pp. 5887–5904. DOI: 10.1023/B:JMSC.0000041686.21788.77.